

Investigation of microwave attenuation and shielding performance of PTFE/Fe₂O₃/OPEFB composites at X-band frequency

M. A. Bello^{a,b}, R. S. Azis^{a,c,*}, M. K. Shabdin^a, N. H. Osman^a, A. Yakubu^d

^a*Department of Physics, Faculty of Science, University Putra Malaysia, 43400 UPM, Serdang, Selangor, Malaysia*

^b*Department of Physics, Shehu Shagari College of Education, Sokoto, P.M.B. 2129, Sokoto, Nigeria*

^c*Nanomaterials Synthesis and Characterization Laboratory (NSCL), Institute of Nanoscience and Nanotechnology (ION2), Universiti Putra Malaysia, 43400 UPM Serdang, Selangor, Malaysia*

^d*Department of Physics, Kebbi State University of Science and Technology, Aliero, Nigeria*

This study explored the microwave attenuation and shielding properties of PTFE/Fe₂O₃/OPEFB composites in the X-band frequency range. Fe₂O₃ nanoparticles were incorporated into the PTFE/OPEFB matrix using a powder-dry mixing technique. The composites were characterized using XRD and FESEM, and attenuation performance was evaluated using a VNA. The results indicated that the addition of Fe₂O₃ nanoparticles improved microwave attenuation and shielding properties, with the composite containing 15 wt% Fe₂O₃ exhibiting the highest attenuation of 16.02 dB. The homogeneous dispersion of Fe₂O₃ nanoparticles was confirmed through FESEM analysis, and XRD analysis confirmed the presence of Fe₂O₃ nanoparticles in the composites. The study concludes that PTFE/Fe₂O₃/OPEFB composites have potential for electromagnetic interference shielding applications in aerospace, telecommunications, and electronics industries.

(Received April 8, 2023; Accepted July 10, 2023)

Keywords: Composites, Microwave Attenuation, Shielding, Fe₂O₃ nanoparticles

1. Introduction

Effective shielding is crucial in engineering applications, which is why selecting materials that provide adequate shielding is essential during design and fabrication. Materials must be able to withstand electromagnetic interference, especially in fields of military hardware, medical applications, telecommunications, and electronics. Typically, polymeric materials are used for casing or packaging in electrical and electronic devices due to their low cost, ease of fabrication, lightweight, and excellent insulating properties. However, plastic was previously only suitable for non-load-bearing general-purpose applications [1–3].

Due to the exceptional qualities of polymers, the scientific community has conducted extensive research on polymeric compounds and substrates [4]. As a result, polymer composites have become a significant contributor to the development of new materials suitable for various applications, including electrical engineering, high-frequency devices such as microwaves, and applications involving shielding, microwave absorption, electromagnetic interference (EMI), electrodes, and sensors [5].

Adding different types of organic or inorganic fillers to polymer systems is a common way to improve their mechanical and electrical properties [6]. Inorganic particles about a micron in size are often used to strengthen polymer matrices so they can better conduct heat and meet mechanical requirements. But the properties of polymer composites are affected by many things, such as the properties of each component, how the fillers touch, how big they are, and what shape they are, as well as how they meet [7].

* Corresponding author: rabaah@upm.edu.my
<https://doi.org/10.15251/DJNB.2023.183.805>

Understanding the behavior of materials in an electromagnetic field is crucial for military hardware, electronics, communication, and industrial applications involving shielding. The measurement of transmission coefficient is commonly used in microwave frequency range applications. Accurate measurement of the transmission coefficient is essential for evaluating the attenuation of materials with good microwave absorption. Attenuation is influenced by several factors, including filler content in the matrix, which is the focus of this study. A proper understanding of these factors is necessary for reliable attenuation measurements.

The combination of PTFE, hematite, and OPEFB in a composite material has not been extensively studied. This study involved the synthesis of PTFE/Fe₂O₃/OPEFB composite structures and the investigation of their electromagnetic propagation and absorption properties at 8–12 GHz. Microwave properties were analyzed using a rectangular waveguide connected to a vector network analyzer via coaxial cable. The attenuation of PTFE/Fe₂O₃/OPEFB composites was examined at different filler contents of 5, 7.5, 10, 12.5, and 15%, while the total volume fraction of the composites was kept constant at 30 g.

2. Materials and method

The PTFE/Fe₂O₃/OPEFB composites were prepared using three different materials. These materials include PTFE matrix powder (purchased from Fujian Sannong New Materials Co., LTD in Sanming, China) with an average particle size ranging from 50–110 µm, Fe₂O₃ nanoparticles with an average particle size of 11.3 nm, and OPEFB fibers (obtained from Ulu Langat Oil Palm Mill in Dengkil, Selangor, Malaysia) with a 75 µm particle size.

2.1. Composites preparation

The fabrication of PTFE/Fe₂O₃/OPEFB samples involved the mixing of varying mass proportions (5–15%) of Fe₂O₃ nanopowder and a constant 5% of OPEFB fiber with a PTFE matrix. The raw materials (Fe₂O₃, OPEFB fiber, and PTFE) were precisely weighed using an analytical microbalance (GR-200, Tokyo, Japan), and then blended into a powder using a wing mixer or blender for 10 minutes. Hydraulic pressing at a pressure of 10 MPa for 5–10 minutes was performed to compact the materials into pellets before sintering. The sintering process began with heating the pellets at a rate of 3 °C per minute from room temperature to 380 °C and holding for 1 h to allow for complete coalescence of the PTFE powder before cooling to room temperature at a rate of 1 °C per minute, as described [8,9]. Table 1 tabulates the composition details used in the fabrication of the composites.

Table 1. Composition of PTFE/Fe₂O₃/OPEFB composites.

PTFE		Fe ₂ O ₃ Nanopowder		OPEFB		Total Mass
(%)	Mass ± 0.05 g	(%)	Mass ± 0.05 g	(%)	Mass ± 0.05 g	Mass ± 0.05 g
90.00	27.00	5.00	1.50	5.00	1.50	30
87.50	26.25	7.50	2.25	5.00	1.50	30
85.00	25.50	10.00	3.00	5.00	1.50	30
82.50	24.75	12.50	3.75	5.00	1.50	30
80.00	24.00	15.00	4.50	5.00	1.50	30

2.2. Characterization

The Fe₂O₃ phase structure and composition, as well as the structures of PTFE, OPEFB fiber, and PTFE/Fe₂O₃/OPEFB composites, were examined in this research using X-ray diffraction (XRD) and a fully automated Philips X-pert system (Model PW3040/60 MPD, Amsterdam, The Netherlands) that operated at a 40.0 kV voltage, a 40.0 mA current, and a 1.5405 nm wavelength with Cu-K radiation. To record the diffraction patterns, the scanning was carried out at a rate of 2°/min over a range of 10 to 70°. All the data were subjected to Rietveld analysis using PANalytical X'Pert Highscore Plus v3.0 software (PANalytical B.V., Almelo, the Netherlands). The surface of the PTFE/Fe₂O₃/OPEFB sample was viewed using a FEI Nova Nano 230 field-emission scanning electron microscope (Kensington FESEM, Sydney, Australia).

The scattering parameters were determined using a rectangular waveguide connected via a high-precision coaxial connection to a network vector analyzer (VNA). The Agilent PNA-L N5227A VNA made by (Agilent Technologies in the United States) was employed in the present study. To ensure the accuracy of the measurement, a full two-port calibration of the instrument's Thru-Reflect-Line (TRL) was performed. This calibration technique efficiently decreases errors resulting from cables and connectors.

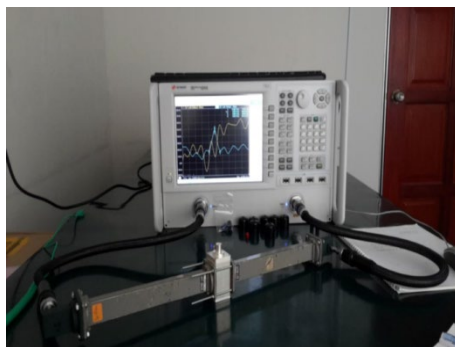


Fig. 1. Experimental arrangement for S parameters measurement.

The terminology used for the scattering parameters is significant. S₁₁ and S₂₂ are referred to as reflection coefficients, while S₁₂ and S₂₁ are known as transmission coefficients. These parameters are directly measurable at microwave frequencies. Typically, S parameters are expressed in complex form [10].

$$S_{gg} = \frac{b_g}{a_g} \quad (g = 1,2) \quad (1)$$

$$S_{pg} = \frac{b_p}{a_p} \quad (p \neq g; p = 1,2; g = 1,2)$$

The reflection coefficient;

$$\Gamma_g = S_{gg} = \frac{b_g}{a_g} \quad (2)$$

The transmission coefficient;

$$T_{g \rightarrow p} = S_{pp} = \frac{b_p}{a_p} \quad (3)$$

Equation (4) uses the transmission coefficients (S₂₁) obtained from the Vector Network Analyzer (VNA) to calculate the attenuation of the material being analyzed.

$$\text{Attenuation (dB)} = -20 \log (S_{21}) \quad (4)$$

2.3. Experimental results

The X-ray diffraction (XRD) patterns of the PTFE/Fe₂O₃/OPEFB composite and the pure OPEFB fiber are shown in Figure 2. The diffractogram of pure OPEFB fiber shows it to be mainly amorphous, but two broad diffraction peaks at 15.72° and 22.43° at 2θ angles indicate the fiber's cellulose crystallinity. The diffraction patterns of the pure PTFE and OPEFB fiber Bragg peaks are visible in the composite's diffraction patterns, and their intensity decreases as the Fe₂O₃ nanofiller concentration increases. This indicates that the composite's crystallinity decreased, which can be attributed to the amorphous OPEFB fiber's inhibition of the PTFE matrix's crystallization, as reported by Icius et al. [11]. Moreover, careful examination of the diffraction patterns revealed that increasing the nanofiller content to 15% transformed the amorphous phases of the PTFE and OPEFB fiber into a single-phase structured material.

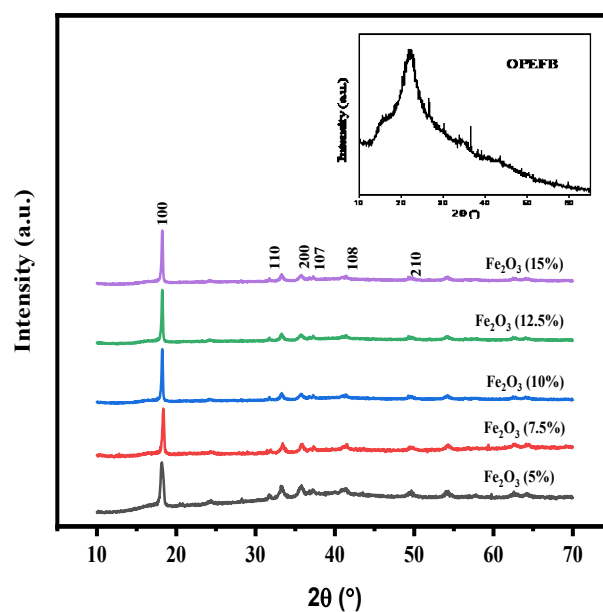


Fig. 2. XRD spectra of PTFE/Fe₂O₃/OPEFB composites

The microstructure of the PTFE/Fe₂O₃/OPEFB composites was analyzed using field emission scanning electron microscopy (FESEM). FESEM micrographs obtained for the 15% nanofiller content are shown in Fig. 3. The FESEM analysis revealed that the hematite particles were well dispersed in the PTFE/OPEFB matrix, and the composite morphology was homogenous. As the hematite content increased, the particle size and distribution became more uniform, leading to an improvement in the microwave absorption properties [12–14]. The composites exhibited a uniform integration of compact Fe₂O₃ nanoparticles throughout the fractured surface, indicating an even reaction between the Fe₂O₃ nanoparticles, OPEFB, and PTFE to form the PTFE/Fe₂O₃/OPEFB composites [1].

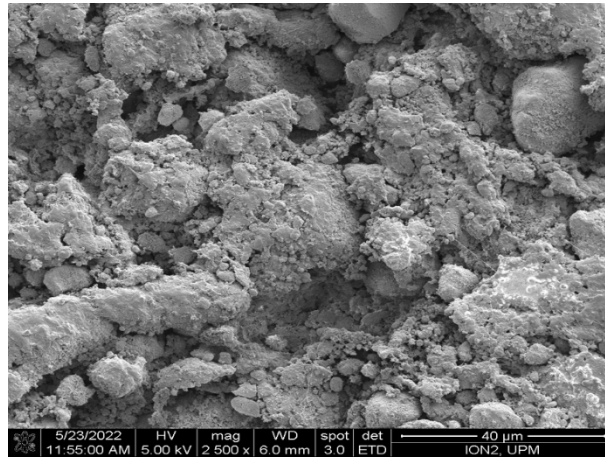


Fig. 3. FESEM micrographs of 15% nanofiller composites.

The obtained data was utilized to plot a graph depicting S_{21} against frequency after conducting the measurements. It is evident that the transmission coefficients decrease sequentially as the Fe_2O_3 nanofiller content increases, as carefully observed in Fig. 4. This observation indicates that the transmission coefficient decreases as the Fe_2O_3 content increases, which is consistent with the theory that denser materials lead to decreased transmission [15]. Additionally, Al-Saleh and Sundararaj [16] reported that the addition of denser materials such as Fe_2O_3 leads to increased attenuation and improved shielding effectiveness.

The composite with the lowest ratio of nanofiller (5% Fe_2O_3) recorded the highest value of transmission coefficients, while the composite with the highest ratio of nanofiller (15% Fe_2O_3) recorded the least value. This finding fits with the impedance mismatch theory, which says that the high permittivity of the nanocomposites makes the electromagnetic wave interact more strongly with the material, causing more absorption and less transmission [17].

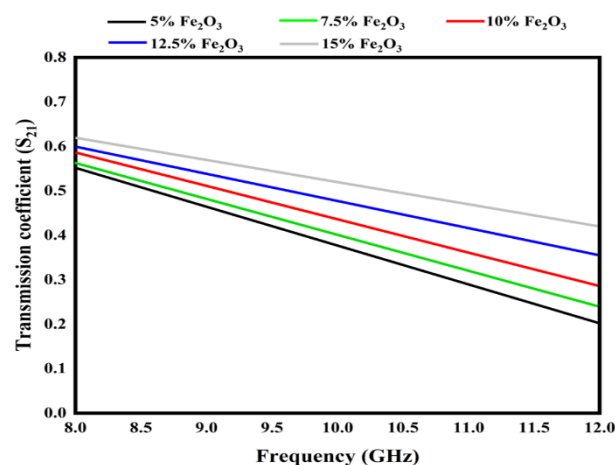


Fig. 4. Measured S_{21} for all the composites.

Fig. 4 showed a decrease in the transmission coefficient of all samples with increasing frequency. The reason for this is the excellent dispersion of the filler in the matrix, which is evident from the uniformity of the particle dispersion in the matrix. Fig. 5 confirms that an increase in filler content led to a reduction in the transmission coefficient magnitude across all frequencies for all filler compositions.

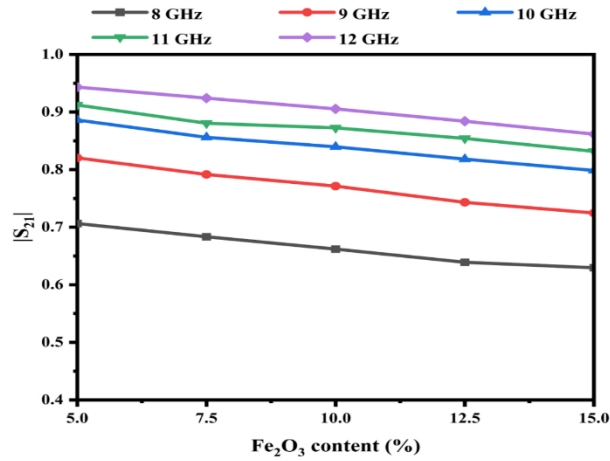


Fig. 5. Transmission coefficients versus Fe₂O₃ nanofiller content.

To calculate the attenuation of the different PTFE/Fe₂O₃/OPEFB pellets, the raw data of the transmission coefficients was used, and Equation (4) was used to calculate the attenuation. The results are presented in Fig. 6a, which shows that the least attenuation was calculated for the 5% Fe₂O₃ nanofiller content, while the highest attenuation was calculated for the 15% nanofiller content. This result is consistent with S₂₁, as the least transmitted composites have the largest absorption. Fig. 6b shows the mean value of attenuation for all filler percentages, which indicates a continued increase in attenuation as the filler content increases. This behavior is consistent with the theory that denser materials decrease transmission [18]. The uniform distribution of the nanofiller in the matrix could have an impact on this phenomenon. If the particles of Fe₂O₃ are evenly dispersed in the matrix, it can either enhance or reduce the attenuation of electromagnetic radiation [18, 19].

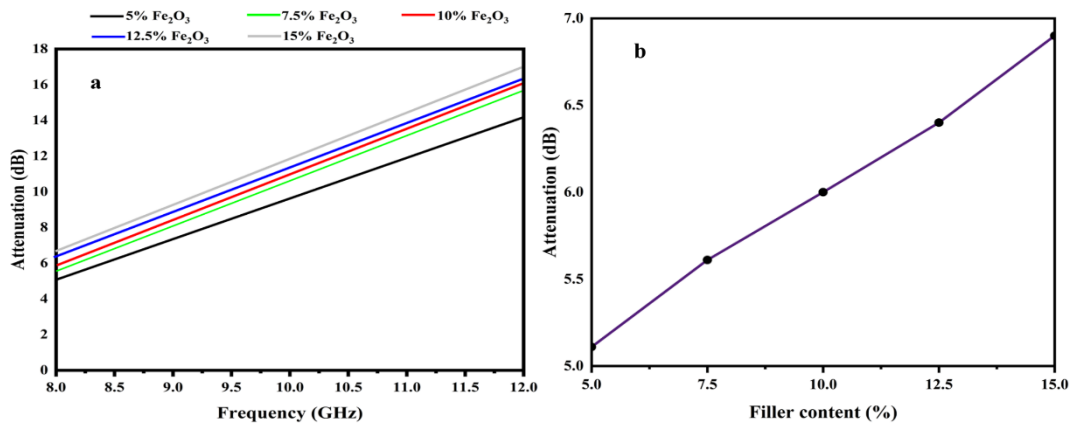


Fig. 6. (a) Calculated attenuation of PTFE/Fe₂O₃/OPEFB composites with various compositions. (b) The mean attenuation of PTFE/Fe₂O₃/OPEFB composites.

3. Conclusion

In this study, PTFE/Fe₂O₃/OPEFB composites were successfully synthesized, and their electromagnetic radiation and material attenuation at X-band frequency were studied. The study focused on analyzing the phase structure, surface morphology, transmission coefficient, and attenuation of the samples. XRD analysis confirmed the presence of Fe₂O₃ nanoparticles in the composites. FESEM analysis revealed a homogeneous dispersion of Fe₂O₃ nanoparticles in the PTFE/OPEFB matrix. The VNA measurements showed that the addition of Fe₂O₃ improved the

microwave attenuation and shielding properties of the composites. The highest attenuation was achieved with the composite containing 15 wt% Fe₂O₃, which showed an attenuation of 16.02 dB. Therefore, it can be concluded that the incorporation of Fe₂O₃ nanoparticles via powder dry mixing technique can effectively enhance the microwave attenuation and shielding performance of PTFE/OPEFB composites at X-band frequency. These composites have potential applications in the development of new and improved materials for electromagnetic interference shielding in the aerospace, telecommunications, and electronics industries.

Acknowledgements

This research was supported financially by the Malaysian Minister of Higher Education and Universiti Putra Malaysia under grant number GP-IPS/2021/9707200.

References

- [1] F. Parres, M. A. Peydro, D. Juarez, M. P. Arrieta, and M. Aldas, *Polymers (Basel)*. 12, 1 (2020); <https://doi.org/10.3390/polym12122974>
- [2] T. Rajamanikandan and S. Banumathi, *Electrochemsci.Org* 16, 21124 (2021); <https://doi.org/10.20964/2021.12.20>
- [3] M. C. Barbu, R. Reh, and A. D. Çavdar, in *Mater. Sci. Eng. Concepts, Methodol. Tools, Appl.* (IGI Global, 2017), pp. 947-977; <https://doi.org/10.4018/978-1-5225-1798-6.ch038>
- [4] I. Delidovich, P. J. C. Hausoul, L. Deng, R. Pfü, M. Rose, and R. Palkovits, (2015).
- [5] E. E. Mensah, Z. Abbas, R. S. Azis, and A. M. Khamis, *Mater.* 2019, Vol. 12, Page 1696 12, 1696 (2019); <https://doi.org/10.3390/ma12101696>
- [6] G. Mittal, K. Rhee, and V. Mišković, *Elsevier* 138, 122 (2018); <https://doi.org/10.1016/j.compositesb.2017.11.028>
- [7] M. Haque, M. Shamsuzzaman, and M. Uddin, *EJERS* 4, 15 (2019); <https://doi.org/10.24018/ejers.2019.4.3.1132>
- [8] I. A. Alhaji, Z. Abbas, M. Hafiz, M. Zaid, N. Zainuddin, and A. M. Khamis, *Myjms.Mohe.Gov.My* 23, 29 (2022).
- [9] A. M. Khamis, Z. Abbas, R. S. Azis, E. E. Mensah, and I. A. Alhaji, *Polym.* 2021, Vol. 13, Page 2332 13, 2332 (2021); <https://doi.org/10.3390/polym13142332>
- [10] A. Yakubu, Z. Abbas, A. Sirajo, A. Yakubu, Z. Abbas, and A. Sirajo, *Open Access Libr. J.* 7, 1 (2020); <https://doi.org/10.4236/oalib.1105444>
- [11] V. Icius De Oliveira Aguiar, M. De Fatima, and V. Marques, *Wiley Online Libr.* 367, 101 (2016); <https://doi.org/10.1002/masy.201500142>
- [12] I. I. Lakin, Z. Abbas, R. S. Azis, and I. A. Alhaji, *Mater.* 2020, Vol. 13, Page 4602 13, 4602 (2020); <https://doi.org/10.3390/ma13204602>
- [13] E. E. Mensah, Z. Abbas, R. S. Azis, N. A. Ibrahim, and A. M. Khamis, 11, 918 (2019); <https://doi.org/10.3390/polym11050918>
- [14] E. E. Mensah, Z. Abbas, R. S. Azis, N. A. Ibrahim, A. M. Khamis, and D. M. Abdalhadi, *Heliyon* 6, e05595 (2020); <https://doi.org/10.1016/j.heliyon.2020.e05595>
- [15] C. Balanis, *Antenna Theory: Analysis and Design* (2015).
- [16] M. H. Al-Saleh and U. Sundararaj, *Carbon N. Y.* 47, 1738 (2009); <https://doi.org/10.1016/j.carbon.2009.02.030>
- [17] R. Deng, M. Li, B. Muneer, Q. Zhu, Z. Shi, L. Song, and T. Zhang, *Materials (Basel)*. 11, (2018); <https://doi.org/10.3390/ma11010107>
- [18] Y. An, Y. Sun, M. Zhang, J. Jiao, D. Wu, T. Wang, and K. Wang, *IEEE Trans. Electron Devices* 65, 4646 (2018); <https://doi.org/10.1109/TED.2018.2863658>

[19] A. Yakubu, Z. Abbas, and S. Sahabi, Glob. J. Mater. Sci. Eng. 1 (2019);
<https://doi.org/10.37516/global.j.mater.sci.eng.2019.0038>

[20] G. Wen, X. Zhao, Y. Liu, H. Zhang, and C. Wang, Chem. Eng. J. 372, 1 (2019);
<https://doi.org/10.1016/j.cej.2010.07.068>